Performance of Hybrid Virtual Force Algorithms on Mobile Deployment in Wireless Sensor Networks

[1]JYH-HORNG WEN, [2]CHENG-CHIH YANG, and [3,*]YUNG-FA HUANG
[1]Department of Electrical Engineering, Tunghai University,
[2]Department of Electrical Engineering, National Chung Cheng University,
[3]Department of Information and Communication Engineering, Chaoyang University of Technology
*168, Jifeng E. Rd., Wufeng District, Taichung, Taiwan
*yfahuang@cyut.edu.tw http://www.cyut.edu.tw/~yfahuang

Abstract: In this paper, three Hybrid Virtual Force Algorithms (HVFA) are proposed to improve the performance of coverage rate, connectivity and energy-efficient moving for dynamic deployment in Wireless Sensor Networks (WSNs). Potential-field-based virtual force algorithm (PF-VFA) can improve the coverage area by distributed mobile deployment. However, the network connectivity performance is degraded due the unevenly node density in WSNs. Therefore, in this paper, a local-density based VFA (LD-VFA) is proposed to improve the network connectivity. Moreover, to further compromise the coverage rate and network connectivity, the sector-density based PF-VFA (PFSD-VFA) is proposed to provide the global density balance. The energy-efficiency of the energy consumption for mobile nodes is considered as one performance metric for sensor dynamic deployment in WSNs. Therefore, a performance combining coverage rate, connectivity, and total moving distance are investigated for the HVFA schemes. Simulation results show that the combing local-density and sector-density VFA (LDSD-VFA) outperform the other VFA schemes.

Keywords: Hybrid virtual force algorithms, coverage rate, network connectivity, local-node-density, sector-node-density, energy-efficiency

1 Introduction

Wireless Sensor Network (WSN) has been proposed for many applications in which the sensors nodes are capable of sensing, computation, and communication [1]. In WSN, sensors deployment builds the network topology. The topology of WSN will decide the performance of networks. Although most of the current WSNs consist of static sensor nodes, there are many applications where mobile nodes are involved [2]. Moreover, due the varying environment and the vulnerable of sensor nodes, the stationary deployment would suffer performance degradation in a long period. Therefore, the dynamic deployment with mobile nodes can adaptively optimized the network topology for WSNs [2-4].

Sensing detection is the main work for WSNs. Binary and probabilistic sensor detection model are two general schemas for sensing activity [5]. Probabilistic sensor detection model is a realistic selection [5].

Integrating multiple nodes deployment, the mainly focuses is how to deploy the sensors reasonably to guarantee a highly-effective on coverage for a Range of Interest (ROI). Coverage area is calculated by grid approach and presented it by contour graph with specific coverage value [6].

Many methods have been developed on the sensors placement and then to improve the coverage rate, such as force field based methods and virtual force algorithms (VFA) [5]. In terms of potential-field-based VFA (PF-VFA) strategy, it models the mobile sensor nodes as the electrons or molecules. The nodes are moved toward or away each other by their virtual forces or potential fields. Then, the VFA can gradually redeploy the position of sensors nodes according to the related nodes density by the virtual repulsive or attractive forces.

In WSN, the higher local node density the higher connectivity. The uniform network topology can prolong the expected system lifetime [7-8]. Thus, the node density affair can be considered to combine the potential-field-based VFA to improve the performance [9-13]. In our works, we propose a local-node-density controlled VFA (LD-VFA) and potential-field-based sector-node-density controlled VFA (PFSD-VFA) to perform effective node deployment.

The rest of this paper is organized as follows. Section 2 describes about probabilistic sensor detection model and coverage rate. Section 3 discusses k-connectivity performance issues for WSNs. The proposed Hybrid Virtual Force Algorithms (HVFA) are illustrated in Section 4. The perform simulation parameters and simulation results are described in Section 5. Section 6 provides some conclusions.

2 Sensing Detection Model and Coverage

2.1 Probabilistic Sensing Detection Model

Sensing detection is a vanguard and essential working in WNS. There are several types of sensing detection model in prior studies, such as binary (disk) and probabilistic sensor detection model [14]. The binary detection model is simple and can facilitate the analysis on network performance. However, it is based on unrealistic assumption of perfect coverage.

To establish a more accurate detection model, probabilistic sensing detection model was proposed using environment actually state [2]. Figure 1 shows the sensing field of an omnidirectional sensor node S_i. Assume that S_i has sensing radius r_s. Then r_e (r_e<r_s) is an uncertainty measure in sensing range. All scope is divided into un-sensing range, uncertain sensing range, and certain sensing range three parts.

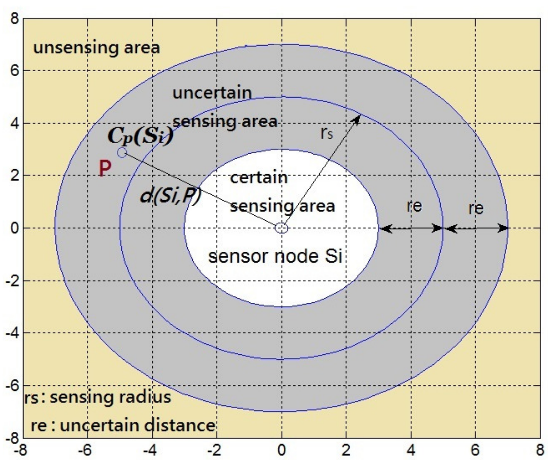

Fig. 1. The sensing field of senor node S_i with sensing coverage probability $C_P(S_i)$

When a point P is located in a sensing field of sensor node S_i, the sensing coverage probability $C_P(S_i)$ is denoted as the detection probability of sensor S_i on point P as shown in Fig. 1. However, in a probabilistic sensing detection model, there is a jump transition of detection probability. An improved probability model ensuring a continuous probability $C_P(S_i)$ is given as [12][15]

$$C_P(S_i)=\begin{cases} 0 & , \quad d(S_i,P)\ge r_s+r_e \\ e^{-\lambda_1\alpha_1^{\beta_1}/\alpha_2^{\beta_2}+\lambda_2} & , r_s+r_e>d(S_i,P)\ge r_s-r_e \\ 1 & , \quad d(S_i,P)<r_s-r_e \end{cases}, \quad (1)$$

where $d(S_i,P)$ is the Euclidean distance between S_i and P, λ_1, β_1, and β_2 are parameters measuring detection probability, $\alpha_1=r_e-r_s+d(S_i,P)$ and $\alpha_2=r_e+r_s-d(S_i,P)$. The disturbing effect λ_2 is omitted in this article. Figure 2 shows contour graph of single sensor node with sensing coverage probability $C_P(S_i)$. From Fig. 2, the contours of C_P =1, 0.7 and 0.4 are depicted.

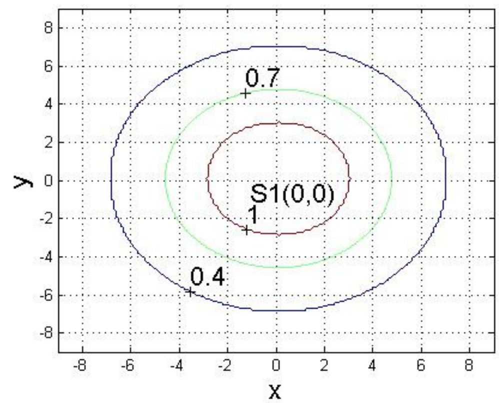

Fig. 2. Contour graph of single sensor node with sensing coverage probability $C_P(S_1)$

2.2 Coverage rate

At first, considering two sensors S_i and S_j in ROI, the probability for detecting a target at point P, $C_P(S_i, S_j)$ can be expressed as [2]

$$C_P(S_i, S_j)=1-(1-C_P(S_i))(1-C_P(S_j)). \quad (2)$$

When the number of nodes is higher than two, we can define a set of sensors by

$$\mathbf{S}_{set}\subseteq\mathbf{S}=\{S_1,S_2,...,S_N\} \ . \quad (3)$$

The sensing coverage probability can be obtained by

$$C_P(\mathbf{S}_{set})=1-\prod\nolimits_{s_i\in\mathbf{S}_{set}}(1-C_P(S_i)) \quad (4)$$

The sensing coverage area estimation is the core working for sensor deployment. By applying grid-based approach, the sensing coverage area (CA) in ROI can be express as

$$CA=\sum\nolimits_{p=1}^{GP}A_p \ , \quad (5)$$

where GP is the number of grid points in sensing field, and

$$A_p = \begin{cases} 1, & C_P(\mathbf{S}_{set}) \geq \theta \\ 0, & C_P(\mathbf{S}_{set}) < \theta \end{cases}, \quad (6)$$

where θ is the coverage probability threshold, $0 \leq \theta \leq 1$. Coverage rate is defined by the ratio of the coverage areas to the area of interest by

$$CR = \frac{CA}{A_{ROI}}, \quad (7)$$

where A_{ROI} is the area of range of interest. Figure 3 shows the contour graph of two sensors deployed at (-5,0) and (5,0), respectively. From Fig. 3, it is seen that the contour is with coverage threshold θ=0.9. With GP=1×1, from (5) the coverage area can be calculated by CA=108. Then from (7) the coverage rate is obtained by CR=0.3375.

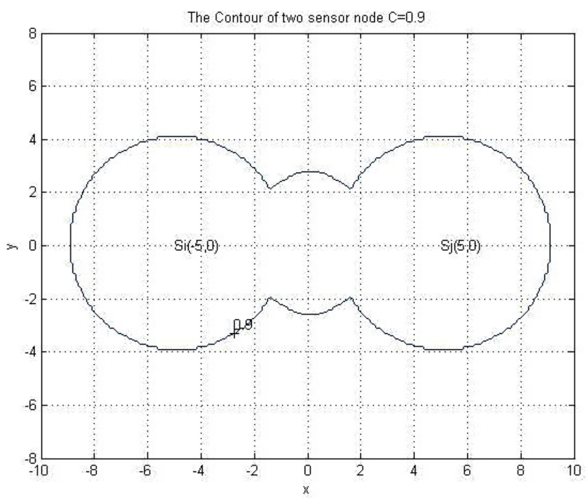

Fig. 3. Contour graph of two sensor nodes

2.3 Coverage Maximization

The optimal nodes deployment can maximize the coverage rate. From Fig. 3, It can be seen that when the distance between two deployed nodes increases to a optimal value, the CA can be maximized [16]. Moreover, when multiple nodes are deployed with unsuitable position, the coverage rate is decreased. Figure 4 shows a specific case that four nodes are located at (-5, 5), (-5, -5), (5, 5), and (5, -5). With θ=0.9, GP=1×1, the coverage area can be calculated by CA=315 from (5). Then from (6) the coverage rate is obtained by CR= =0.35, with A_{ROI}=900. In Fig. 4, there exists a coverage hole in contour graph. Thus, there exist the monitored faults in non-full-coverage sensing field [16].

In the maximization of coverage area, the optimal distance between two nodes can be decide by greedy algorithm by the given coverage threshold θ as shown in Fig. 5.

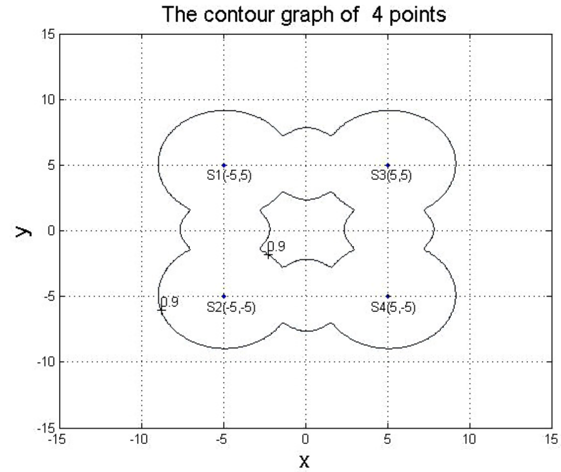

Fig. 4. Contour graph of 4 sensors exist a coverage hole.

To be simplified, an approximated distance threshold d_{th} is used to decide the distance between the sensors to obtain the higher coverage area in WSN. Figure 5 shows the optimal d_{th} =1.9×r_s by greedy algorithm for two sensor nodes. For multiple nodes and full-coverage sensing field, the distance threshold $d_{th} = \sqrt{3} \cdot r_s$ is adopted in this paper [5].

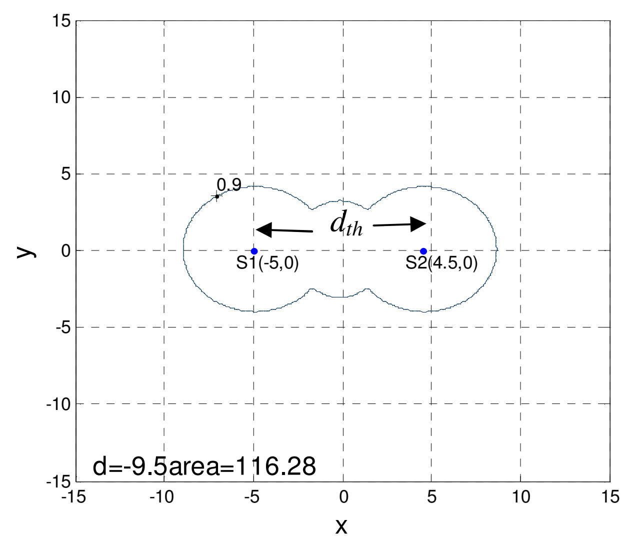

Fig. 5. The d_{th} optimization for two nodes deployment.

3 *k*-Connectivity Network

3.1 Neighbor-Based Topologic Control

Neighbor-based topologic control is one of important methods for distributed deployment in WSNs which rely on nodes' ability to determine the number and identity of neighbors within the maximum transmitting range [17]. Liu and Li try to make the number of neighbors of each node beyond a threshold [17]. When the actual number of neighbors is higher than the threshold, the transmitting range is increased, until the number of neighbors reaches the desired value. However, the higher transmitting range will consume more energy foe the nodes with less neighbors.

3.2 Network Connectivity

Network connectivity is one of important performance metrics. Sensor networks need to remain enough connection and improve information collection of sensor nodes.

In a k-connectivity ($k \geq 1$) wireless communication networks, there are at least k disjoint connection for each sensor node S_i.

Let **S** be a set of all sensors in ROI. The set of neighbor nodes of the ith node in AOI can be defined by $\mathbf{S}_{ni}=\{S_j \in \mathbf{S}, \mid d_{ij} \leq r_c, j \neq i\}$, where d_{ij} is Euclidean distance between S_i and S_j. The number of neighbor nodes of S_i is denoted as N_{ni}, which is defined as local-density of S_i. Therefore, the k-connectivity means that there are at least k neighbor nodes for each node.

The OGDC [18] was proposed to derive the necessary and sufficient condition under a desired coverage and connectivity performance. The communication range r_c is decided by at least twice of the sensing range r_s, by $r_c \geq 2r_s$.

Moreover, Santi [19] proposed a critical communication range r_{cc} in a dense network. Under the hypothesis that nodes are uniformly distributed in $[0,1]^2$ space, the r_{cc} for connectivity with high probability is obtained by

$$r_{cc} = \sqrt{\log N / N} \,. \tag{8}$$

It is only sufficient condition but not necessary. The characteristic curve of (8) is shown in Fig. 6 with the area of ROI A_{ROI}=60×60. From Fig. 6, it is shown that with N=70, r_{cc}≈10 can obtain connectivity with high probability.

The performance of network connectivity can derived from average neighbor node density (*ANND*) which is the average number of neighbor nodes, expressed by

$$ANND = \frac{1}{N}\sum_{i=1}^{N} N_{ni} \ , \tag{9}$$

where N_{ni} is the number of neighbors of ith node. Moreover, a connectivity uniformity of U_c can be expressed by

$$U_c = \sqrt{\frac{1}{N}\sum_{i=1,}^{\mathrm{N}} (nn_i - \mu)^2} \ , \tag{10}$$

where μ is the average node density of networks. The U_c is also the standard deviation of node local densities with expected local density. The *ANND* is an index of network connectivity. However, to be generalized, a performance of connectivity index (CI) of networks is defined by

$$CI = \frac{ANND}{\mu} \,. \tag{11}$$

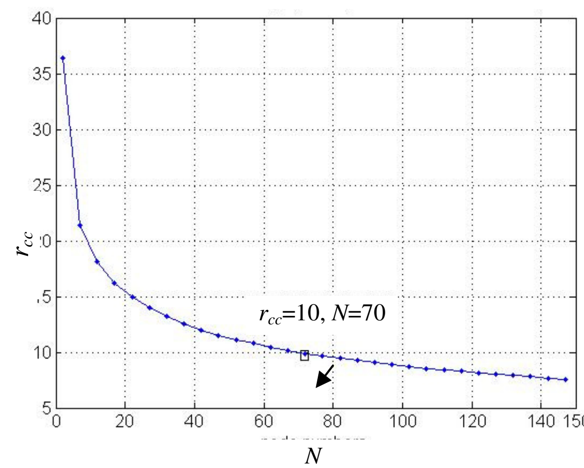

Fig. 6. r_{cc} vs. sensor number connectivity with high probability

4 Hybrid Virtual Force Algorithm

Three HVFA schemes are proposed to compare with PF-VFA. The proposed schemes include LD-VFA, PFSD-VFA and LDSD-VFA to investigate the deployment optimization based on the nodes density information.

4.1 Potential- Field Based Virtual Force

Zou [5] combined the potential-field based algorithm and the disc coverage theory by abstracting the sensor node to be a particle in the potential field, where the repulsive forces exits between each pair of the nodes. The total resultant force exerted on sensor node n_i is denoted as $\boldsymbol{F}_i$ by

$$F_i = \sum_{j=1, j\neq j}^{k} F_{ij}^P \ , \tag{12}$$

where $\boldsymbol{F}_{ij}^{P}$ is the force exerted by n_j, expressed by

$$F_{ij}^P = \begin{cases} w_r(d_{th} - d_{ij}) \cdot \alpha_{ji} & , \ d_{ij} < d_{th} \\ 0 & , \ d_{ij} \geq d_{th} \end{cases} \ , \tag{13}$$

where w_r represents the virtual repulsive force coefficients, α_{ij} is the angle between node S_i and node S_j, $\alpha_{ji} = -\alpha_{ij}$. An exponential factor is applied to smooth the function curve by

$$\alpha_{ij} = e^{-\lambda_1 \alpha_1^{\beta_1} / \alpha_2^{\beta_2}} \ , \tag{14}$$

where λ_1, α_1, α_2, β_1 and β_2 are parameters measuring detection probability. Then, the characteristic curve of F_{ij}^P vs. d_{ij} with d_{th} =10.can be shown in Fig. 7. In this paper, only surround neighbor nodes is considered with ignoring other interested and obstacles region.

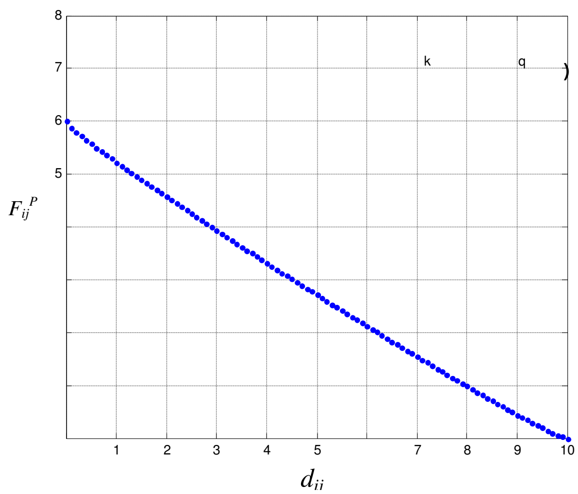

Fig. 7. Characteristic curve of F_{ij} vs. d_{ij} with d_{th} =10.

4.2 Local-Density Based VFA

The VFA can move the near sensor node to increase the distance and make the uniformly topology. The virtual force only depend the distance between the nodes. However, when the nodes deployed with a dense area, the repulsive force should be higher to move the nodes faster than that of a sparse area. Therefore, we combining the local-density and VFA scheme to effectively move the uneven nodes.

An expected density is defined by

$$\mu = \frac{N\pi \cdot r_c^2}{A_{ROI}} \ . \tag{15}$$

where N is the number of sensor nodes in ROI.

The uniform distribution of nodes is a main prospect for high coverage rate. Therefore, the number of neighbors of nodes can be counted as the node local-density. Then we combine the node local-density to VFA, the repulsive effect can be enhanced when node local-density is higher than expected density μ in (11). Thus, the local-density virtual force F_i^D can be obtained by

$$F_i^D = \sum_{j=1, j\neq i}^{N} F_{ij}^D \ , \tag{16}$$

where F_{ij}^D is the force exerted on node S_i by node S_j with LD-VFA, in which is obtained by combining the local-density and VFA as

$$F_{ij}^D = \begin{cases} \frac{N_{ni}}{\mu} \times F_{ij}^P, \ N_{ni} \geq \mu \\ F_{ij}^P \quad , \quad N_{ni} < \mu \end{cases} , \tag{17}$$

where F_{ij}^P is the force exerted on node S_i by node S_j with PF-VFA. Figure 8 shows an example of the $\boldsymbol{F}_{ij}^{D}$ of local-density virtual force.

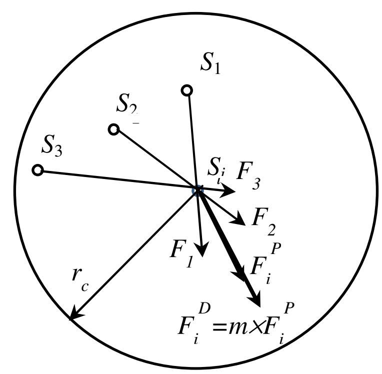

Fig. 8. Local density virtual force $\boldsymbol{F}_{ij}^{D}$

4.3 Sector-Node-Density VFA

The effective virtual force of LD-VFA is dominated by local area surrounding the forced node. However, the node density variety in global area can be consider to enhance the virtual force in global view. Thus, in this paper, the area of ROI is divided to 4 sectors. Each sector can be given a sector node-density (*SND*).

Then the hybrid virtual force active on sensor node S_i can be express as

$$F_i^H = F_i + F_i^S \tag{18}$$

where F_i is total virtual force of PF-VFA, $F_i^S = f(SND_x)$ is the sector-density virtual force. Figure 9 shows a four-sector architecture of AOI. From Fig. 9, it is easy to know that the density of each sector would be different. Then the virtual force in different sector should be different to balance the moving speed for AOI.

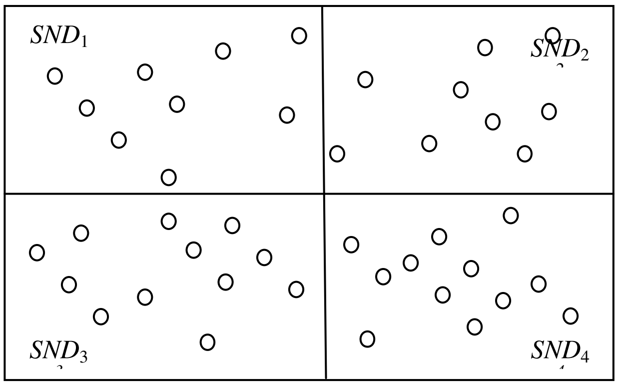

Fig. 9. Four sectors ROI for LDSD-VFA scheme.

4.4 Summary of Hybrid Virtual Force Algorithm

The simulation on the HVFAs can be described as the procedures in one round as shown in Fig. 10.

Begin
System initialized
  Sensor node deploy randomly $\{S_1, S_2, ---, S_N\}$
  Parameter setting $\{ r_s, r_c, r_e, d_{th}, , N, \mu\}$
  Sector node density estimate $\{S_{ND1}, S_{ND2}, \ldots, S_{NDz}\}$.
For i=1 to N
  Find all neighbors for sensor node S_i
    $N_{ni}=k$
  Potential- Field Virtual Force computing
    $F_i = \sum_{j=1, j\neq i}^{N_{ni}} F_{ij}^P$
  Local-Density Virtual Force computing
    $F_i = \sum_{j=1, j\neq i}^{N_{ni}} F_{ij}^D$
  Sector-Node-Density Virtual Force computing
    $F_i^S = f(S_{NDi})$
  Total Virtual Force computing
    $F_i^H = F_i + F_i^S$
End For
All sensor nodes moving to a new location simultaneously after a period time
Performances evaluation
End

Fig. 10. Procedures for Hybrid Virtual Force Algorithms

4.5 Energy Efficiency for Dynamic Deployment

In a deployment round, all mobile sensor nodes execute virtual force procedures and move to new locations simultaneously in a period time τ. Let $(X_{\tau i}, Y_{\tau i})$ be the location of node S_i at the τ-th round. We can express the moving distance $d_{\tau i}$ of node S_i after the τ-th round as

$$d_{\tau,i} = \sqrt{(X_{\tau,i} - X_{\tau-1,i})^2 + (Y_{\tau,i} - Y_{\tau-1,i})^2} . \tag{19}$$

Total moving distances (TMD) means all nodes moving sum after virtual force effective, which is defined as

$$TMD = \sum_{\tau=1}^{w}\sum_{i=1}^{N} d_{\tau,i} , \tag{20}$$

where N is node total numbers. w is the time periode when system stable. Because the node moving needs power consumption, TMD is related with energy consumption. Therefore, to investigate the energy efficiency for dynamic deploments for WSNs, an index of moving power consumption (MPCI) can be obtained in terms of TMD by

$$MPCI = 1 - \frac{TMD}{TMD_{Max}} , \tag{21}$$

where TMD_{max}, maximum and transfer TMD as a moving power consumption index.

Moreover, to compromize the performance of coverage rate, connetivity and moving energy-efficiency, a synthesizing peformance index, SPI, is defined as

$$SPI = \sqrt{CR^2 + CI^2 + MPCI^2} . \tag{22}$$

5 Simulation and Results

The parameters for simulation environments are listed in Table 1. Initially, we randomly deploy 50 nodes in sensing field. The PF-VFA is performed to investigate the virtual impulsive force.

Figure 11 shows the nodes' locations with randomly deployment. From Fig. 11, it is eazily seen that there are some dense area and some soarse area. After three ronnds deployment by PF-VFA, the location distribution of nodes is shown in Fig. 12. From Fig, 12, it is observed that the loacation distribution of nodes is more uniform than that initial deployment in Fig. 11.

To further investigate the relation between CR and N, the results of coverage rate with PF-VFA is performed for the number of nodes N=50-100 as shown in Fig. 13. From Fig. 13, it is seen that at N=50, the CR=0.75. When the total number of nodes N increases from 50 to 100, coverage rate increases from 0.75 to 0.995.

Table 1. Simulation parameters

Parameters	**Values**
Sensing field, A_{ROI}	60×60 (m^2)
Total number of nodes, N	50-100
Transmission range, r_c	10 (m)
Sensing range, r_s	5 (m)
Sensing threshold, d_{th}	9 (m)
Sensing coverage threshold, θ	0.9
Performance index	CA, CR, CI, TMD, MPCI, SPI

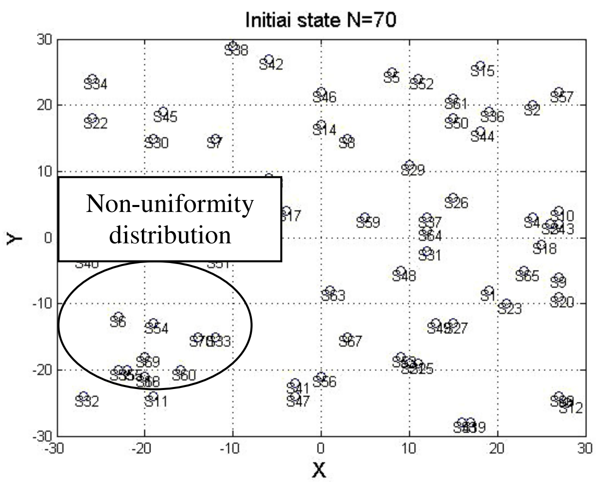

Fig. 11. The location distribution of nodes at initially deployments.

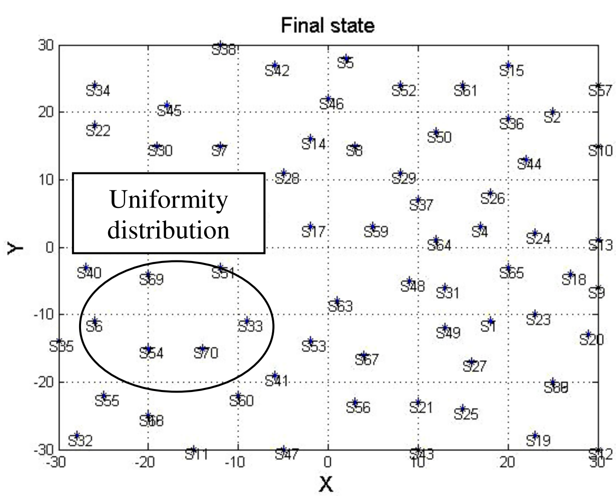

Fig. 12. The location distribution of nodes after VFA operation.

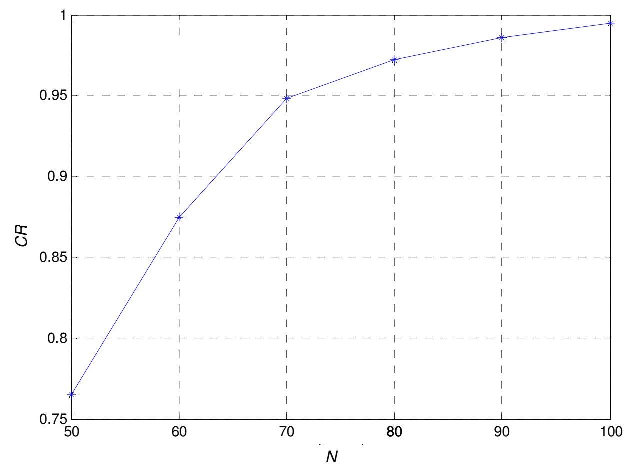

Fig. 13. The relation of coverage rate v.s. the number of nodes for PF-VFA scheme.

Figure 14 shows average neighbor node density for various VFAs. From Fig. 14, it is observed that the ANND becomes lowest at the third round in PF-VFA. That is because that in the dense area of PF-VFA, the total virtual force are higher to move nodes to spread out to the sparse area. However, the LDSD-VFA can balance both the local and global virtual force to gradually move the nodes and has the highest average neighbor node density than other schems.

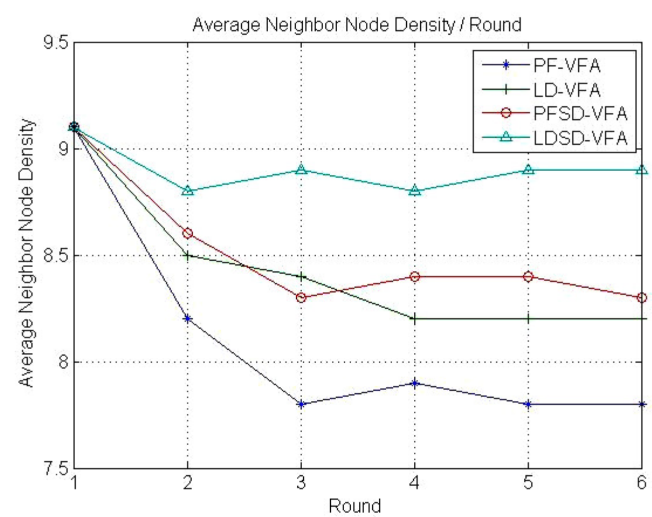

Fig. 14. The comparisons of average number of neighbor nodes in each rounds for HVFAs.

To investigate the energy efficiency, in each round the TMD of HVFAs are compared in Fig. 15. From Fig. 15, it is observed that the TMD of PF-VFA is the largest amon the HVFAs. In the LD-VFA, the node movement is the slowest among the HVFAs.

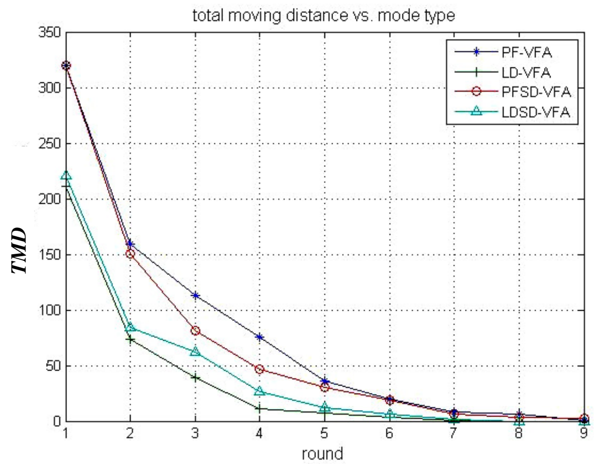

Fig. 15. The comparisons of TMD at each rounds for HVFAs.

The performance comparisons for HVFAs are shown in Table 2 with *N*=100 and the third round. The HVFAs includes PF-VFA, LD-VFA, SD-VFA and LDSD-VFA schemes. From Table 2, it is shown that PF-VFA obtains the best *CA* and *CR*. Then, in the coverage performance the PF-VFA outperforms the other three HVAF schemes. However, the proposed HVFAs outperforms PF-VFA in connectivity and energy-consumption performance. The sectorrized diversity of LDSD-VFA scheme can effectively obtain the globel optimization for the connectivety rate. The effective location of globelized deployment in LDSD-VFA can largely outperform other PF-VFA schemes on the performance of TMD. Thus, the proposed LDSD-VFA scheme exhibits the best performance of SPI.

Table 2. Comparisons of HVFAs on coverage rate, connectivity and energy consumption .

Index \ HVFA		PF-VFA	LD-VFA	PFSD-VFA	LDSD-VFA
Cover-age	*CA*	3512.3 (m^2)	3455.7 (m^2)	3457.3 (m^2)	3392.7 (m^2)
	CR	0.98	0.96	0.96	0.94
Connec-tivity	*ANND*	7.7	8.3	8.3	8.8
	CI	0.88	0.95	0.95	1.01
Energy Consu-mption	*TMD*	739.0	345.9	659.5	413.4
	MPCI	0.26	0.65	0.34	0.59
SPI		1.340	1.499	1.390	1.503

Figures 16 and 17 show performance comparisons of HVAFs. From Fig. 16, even though the CR performance of the PF-VFA is the best, the CI of the PF-VFA is the worst than other HVFAs. Morever, the TMD performance of the proposed LD-VFA is superier to the others. Therefore, from Fig. 17, it is seen that both LD-VFA, and LDSD-VFA schemes outperform the others of PF-VFA, and PFSD-VFA in SPI.

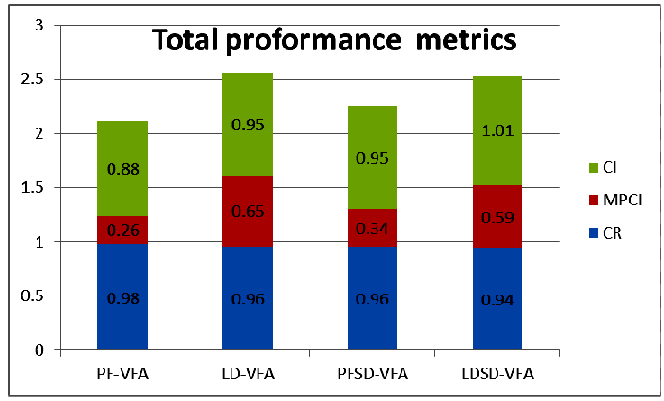

Fig. 16. Performance comparison on CR, MPCI and CI for HVFAs.

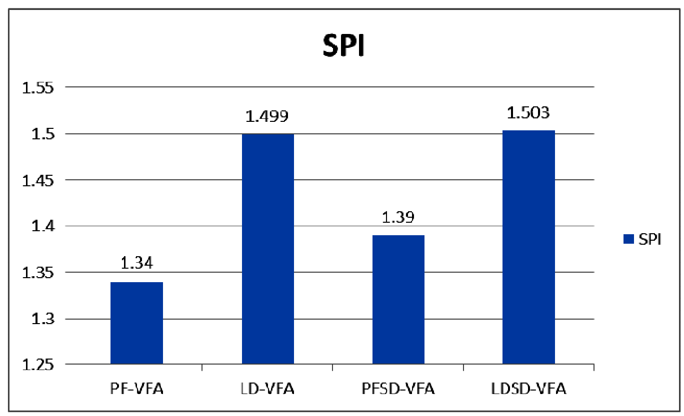

Fig. 17 The performance comparions of SPI for HVFAs.

6 Conclusion

In this paper, the HVFA schemes are proposed to improve performance of coverage rate, connectivity, and moving power consumption for nodes dynamic deployment in WSNs. The local-density of AOI is proposed to combine the VFA to largely improve the network connectivity performance, The sector-density is proposed to compromise the local and global optimization for the dynamic deployments. Simulation results show that the proposed HVFA outperforms PF-VFA approach especially in energy-efficiency of dynamic nodes moving. Furthermore, the sector diversity of LDSD-VFA scheme can effectively obtain the globel optimization for the connectivety rate. The effective location of globelized deployment in LDSD-

VFA can largely outperform other PF-VFA schemes on the performance of TMD. Thus, the proposed LDSD-VFA scheme exhibits the best performance of SPI.

Reference

[1] I. F. Akyildiz, S. Y. Sankarasubramaniam, and E. Cyirci, "Wireless Sensor Networks: A Survey," *Computer Networks*, Vol. 38, No. 4, pp. 393-422. , 2002

[2] A. Howard, M. J. Mataric and G. S. Sukhatme, "Mobile Sensor Network Deployment Using Potential Fields: A Distributed, Scalable Solution to the Area Coverage Problem," In *Proceedings of 6th Int. Conf. Distributed Autonomous Robotic System*, Fukuoka, Japan, pp. 299-308, 2002.

[3] N. Thangadurai, R. Dhanasekaran and R. D. Karthika, "Dynamic Energy Efficient Topology for Wireless Ad hoc Sensor Networks," *WSEAS Transactions on Communications*, Vol. 12, Issue 12, pp. 651-660, December 2013.

[4] D. G. Costa, L. A. Guedes, F. Vasques and P. Portugal, "Redundancy-Based Semi-Reliable Packet Transmission in Wireless Visual Sensor Networks Exploiting the Sensing Relevancies of Source Nodes," *WSEAS Transactions on Communications*, Vol. 12, Issue 9, pp. 468-478, September 2013.

[5] Y. Zou and K.Chakrabarty, "Sensor Deployment and Target Localization Based on Virtual Forces," In *Proceedings of IEEE INFOCOM*; pp. 1293– 1303, 2003.

[6] P. Gao, W.-R. Shi, H.-B. Li, W. Zhou, "Indoor Mobile Target Localization Based on Path-planning and Prediction in Wireless Sensor Networks," *WSEAS Transactions on Computers*, Vol. 12, Issue 3, pp. 116-127, March 2013.

[7] N. Heo and V. P. Kumar, "A distributed self spreading algorithm for mobile wireless sensor networks," In *Proceedings of IEEE WCNC* , pp. 1597 – 1602, 2003.

[8] K. P. Sampoornam and K. Rameshwaran, "An Efficient Data Redundancy Reduction Technique with Conjugative Sleep Scheduling for Sensed Data Aggregators in Sensor Networks," *WSEAS Transactions on Communications*, Vol. 12, Issue 9, pp. 499-508, September 2013.

[9] C. Liu, and J. Wu, "Virtual-Force-Based Geometric Routing Protocol in MANETs," *IEEE Transactions on Parallel and Distributed Systems*, vol. 20 , Issue 4, pp. 433 – 445, 2009.

[10] M. Parameswaran, V. Rastogi, and C. Hota, "A Virtual-Force Based Multicast Routing Algorithm for Mobile Ad-Hoc Networks," In *Proceedings of 2013 Fifth International Conference on Ubiquitous and Future Networks (ICUFN)*, pp. 696 – 700, 2013.

[11] X. Yu, W. Huang, J. Lan, and X. Qian, "A Novel Virtual Force Approach for Node Deployment in Wireless Sensor Network," In *Proceedings of 2012 IEEE 8th International Conference on Distributed Computing in Sensor Systems (DCOSS)*, pp. 359-363, 2012.

[12] S. Li, C. Xu, W. Pan, and Y. Pan "Sensor Deployment Optimization for Detecting Maneuvering Targets," In *Proceedings of 2005 7th International Conference on Information Fusion* 1629-1635.

[13] N. Bartolini, G. Bongiovanni, T. La Porta, and S. Silvestri, "On the Security Vulnerabilities of the Virtual Force Approach to Mobile Sensor Deployment," In *Proceedings of 2013 IEEE INFOCOM,* pp. 2418 – 2426, 2013.

[14] N. Ahmed, S. S. Kanhere, and S. Jha, "Probabilistic Coverage in Wireless Sensor Networks," In *Proceedings of IEEE Conference on Local Computer Networks (LCN'05)*, pp. 672-681, Sydney, Australia, Nov. 2005.

[15] J. Li, B. Zhang, L. Cui, and S. Chai, "An Extended Virtual Force-based Approach to Distributed Self-Deployment in Mobile Sensor Networks," *International Journal of Distributed Sensor Networks*, 2012.

[16] S. Meguerdichian, F. Koushanfar, M. Potkonjak, and M. Srivastava, "Coverage Problems in Wireless Ad-Hoc Sensor Network," In *Proceedings of IEEE INFOCOM*, 2001.

[17] J. Liu, and B. Li, "Mobilegrid: Capacity-Aware Topology Control in Mobile Ad Hoc Networks," In *Proceedings of IEEE International Conference on Computer Communications and Networks*, pp. 570–574, 2002.

[18] H. Zhang and J. Hou, "Maintaining Sensing Coverage and Connectivity in Large Sensor Networks," *Ad Hoc and Sensor Wireless Networks: An International Journal*, Vol. 1, No. 1-2, pp. 89–123, January 2005.

[19] P. Santi, "Topology Control in Wireless Ad Hoc and Sensor Networks," *ACM Computing Surveys*, Vol. 37, No. 2, June 2005.